SIAM J. SCI. COMPUT.
Vol. 41, No. 2, pp. B274–B294

A NUMERICAL MODE MATCHING METHOD FOR WAVE SCATTERING IN A LAYERED MEDIUM WITH A STRATIFIED INHOMOGENEITY*

WANGTAO LU†, YA YAN LU‡, AND DAWEI SONG§

Abstract. Numerical mode matching (NMM) methods are widely used for analyzing wave propagation and scattering in structures that are piecewise uniform along one spatial direction. For open structures that are unbounded in *transverse directions* (perpendicular to the uniform direction), the NMM methods use the perfectly matched layer (PML) technique to truncate the transverse variables. When incident waves are specified in homogeneous media surrounding the main structure, the total field is not always outgoing, and the NMM methods rely on reference solutions for each uniform segment. Existing NMM methods have difficulty handing grazing incident waves and special incident waves related to the onset of total internal reflection, and are not very efficient at computing reference solutions for nonplane incident waves. In this paper, a new NMM method is developed to overcome these limitations. A hybrid Dirichlet-Robin boundary condition is proposed to ensure that nonpropagating and nondecaying wave field components are not reflected by truncated PMLs. Exponential convergence of the PML solutions based on the hybrid Dirichlet–Robin boundary condition is established theoretically. A fast method is developed for computing reference solutions for cylindrical incident waves. The new NMM is implemented for two-dimensional structures and polarized electromagnetic waves. Numerical experiments are carried out to validate the new NMM method and to demonstrate its performance.

Key words. mode matching method, perfectly matched layer, wave scattering, layered medium

AMS subject classifications. 78A40, 78M25, 65L15

DOI. 10.1137/18M1182693

1. Introduction.

Wave scattering problems in a layered medium with a penetrable or impenetrable inhomogeneity appear in numerous scientific and engineering applications [9]. Classical numerical methods such as the finite difference method, the finite element method (FEM) [23], and the spectral method are very versatile but are not always the most efficient, since they need to discretize the whole computational domain. For piecewise homogeneous structures, the boundary integral equation (BIE) methods [7, 6, 17, 21] are highly competitive since they discretize only the interfaces and the boundary of the inhomogeneity. If the structure can be divided into a number of segments or regions where the governing equation becomes separable, the mode matching method [9], also known as the mode expansion method or modal method [5, 19, 26], can be used. The mode matching method has many numerical invariants in various applications, including the Fourier modal methods [12, 13, 16, 18, 20], a Legendre/Chebyshev polynomial expansion modal method [24], and the pseudospectral modal methods [10, 29] in analyzing diffraction gratings, the propagator-matrix based modal method [11] and the two-stage semianalytic modal method [3, 4] in

*Submitted to the journal's Computational Methods in Science and Engineering section April 23, 2018; accepted for publication (in revised form) February 14, 2019; published electronically March 28, 2019.

http://www.siam.org/journals/sisc/41-2/M118269.html

Funding: The second author was partially supported by the Research Grants Council of Hong Kong Special Administrative Region, China (grant CityU 11304117).

†School of Mathematical Sciences, Zhejiang University, Hangzhou 310027, China (wangtaolu@zju.edu.cn).

‡Department of Mathematics, City University of Hong Kong, Kowloon, Hong Kong (mayylu@cityu.edu.hk).

§Department of Mathematics, Nanjing University of Aeronautics and Astronautics, Nanjing, Jiangsu, China (dwsmath@nuaa.edu.cn).

analyzing waveguides, and more recently the vertical mode expansion method [22] in analyzing wave scattering upon a slab, etc.

Typically, these methods are applicable if the structure is piecewise uniform along one spatial direction. In each uniform segment, the wave field is expanded in eigenmodes of a differential operator in the *transverse variable* (whose axis is perpendicular to the uniform spatial direction), and the expansion coefficients are solved from a linear system obtained by matching the wave field at the interfaces between neighboring segments. The classical mode matching method solves the eigenmodes analytically. The numerical mode matching (NMM) methods solve the eigenmodes by numerical methods, and they are easier to implement and applicable to more general structures. In comparison with some standard numerical methods like FEM method, the mode matching method and its variants have the advantage of avoiding discretizing one spatial variable. They are widely used in engineering applications, since many designed structures are indeed piecewise uniform.

For numerical simulations of waves, the perfectly matched layer (PML) [2] is an important technique for truncating unbounded domains. It is widely used with standard numerical methods, such as FEM, that discretize the whole computational domain. The BIE methods usually automatically take care of the radiation conditions at infinity, but for scattering problems in layered media, PML can also be used to efficiently truncate interfaces that extend to infinity [21]. For NMM methods, PML was first applied to study piecewise uniform waveguides [11, 3, 4]. An optical waveguide is an open structure, i.e., the transverse domain perpendicular to the waveguide axis is unbounded. The analytic mode matching method is difficult to use, since the transverse operator has a continuous spectrum and field expansions contain integrals related to the radiation modes. When a PML is used to truncate the transverse domain, typically with a zero Dirichlet boundary condition at the external boundary of the PML, the continuous spectrum is discretized, and the field expansions are approximated by sums of discrete eigenmodes.

For many applications, an incident wave is specified in the homogeneous media surrounding the scatterer; then the total wave field in each uniform segment does not satisfy outgoing radiation conditions in the transverse directions and is incompatible with the eigenmodes computed using a PML. To overcome this difficulty, we can find a reference solution for the given incident wave in each uniform segment and then expand the difference between the total field and the reference solution in the PML-based eigenmodes [22]. Typically, the field difference in each segment is indeed outgoing in the transverse directions, and an NMM method based on this approach works reasonably well. But unfortunately, the method breaks down in special circumstances where the field difference in a segment contains a component that is exactly or nearly invariant in the transverse direction, i.e., a component with a zero or near zero transverse wavenumber. This happens if the incident wave has the critical incident angle for the onset of total internal reflection in the exterior segments. In that case, the field difference in any interior segment contains a nonpropagating and nondecaying component with a zero or near zero transverse wavenumber. This difficulty also arises when the incident wave is nearly parallel to the uniform direction, i.e., a grazing incidence. In that case, the field difference in an interior segment also contains a plane wave component with a near zero transverse wavenumber.

In this paper, we develop a new NMM method to overcome the above difficulty. Our approach is to use a Robin boundary condition for the PML in the interior segments. The boundary condition is designed to ensure that the field component with a zero or near zero transverse wavenumber is not reflected by the PML. A similar Robin-type condition for PML was previously used by one of the authors to preserve a weakly confined guided mode propagating in optical waveguides [14]. For the exterior segments, we keep the simple zero Dirichlet boundary condition. To give the method a theoretical foundation, we analyze the effectiveness of the PML using such a hybrid Dirichlet–Robin boundary condition. It is shown that the error induced by the PML decays exponentially with the thickness or the absorbing coefficient of the PML. For scattering problems with incident waves from a point or line source, the NMM method faces an additional difficulty, namely, the computation of the reference solutions, especially for the segment involving the inhomogeneity. The traditional approach that turns a point or line source to plane waves by Fourier transform is not very efficient. We develop an efficient method for computing the reference solutions based on the PML technique and the method of separation of variables.

The rest of this paper is organized as follows. In section 2, we formulate the scattering problem and review the PML theory. In section 3, we describe an NMM method. In section 4, we derive the new Robin-type boundary condition and show that the solution based on a PML and a hybrid Dirichlet–Robin condition converges to the true scattering solution exponentially. In section 5, we develop an efficient method for computing reference solutions when the incident wave is a line source. In section 6, we present a few numerical examples to validate our NMM method and to illustrate its performance. The paper is concluded by some remarks and discussions in section 7.

2. Problem formulation. To simplify the presentation, we begin with a scattering problem in a two-layer medium. As shown in Figure 1(a), the physical structure is characterized by a z-invariant dielectric function

$$\varepsilon(x,y) = \begin{cases} \varepsilon_+ = n_+^2, & (x,y) \in \mathbb{R}_+^2 \backslash \bar{D}, \\ \varepsilon_D(y), & (x,y) \in D, \\ \varepsilon_- = n_-^2, & (x,y) \in \mathbb{R}_-^2 \backslash \bar{D}, \end{cases} \tag{1}$$

where $\mathbb{R}_\pm^2 = \{(x,y) \in \mathbb{R}^2 : \pm y > 0\}$, $\varepsilon_D(y) \geq 1$ is smooth on (y_0, y_1), D is a rectangle $(-x_0, x_0) \times (y_0, y_1)$ with $x_0 > 0$, $y_1 \geq 0$ and $y_0 \leq 0$, and it corresponds to a stratified inhomogeneity.

In $\mathbb{R}_+^2 \backslash \bar{D}$, we specify a plane incident wave $u^{\rm inc} = e^{i(k_\rightarrow x - k_\uparrow y)}$, where the x-wavenumber $k_\rightarrow = k_0 n_+ \sin\theta$, the y-wavenumber $k_\uparrow = k_0 n_+ \cos\theta$, and $\theta \in (-\pi/2, \pi/2)$ is the incident angle. The total wave field $u^{\rm tot}$ satisfies the Helmholtz equation

$$\Delta u^{\rm tot} + k_0^2 \varepsilon(x,y) u^{\rm tot} = 0, \tag{2}$$

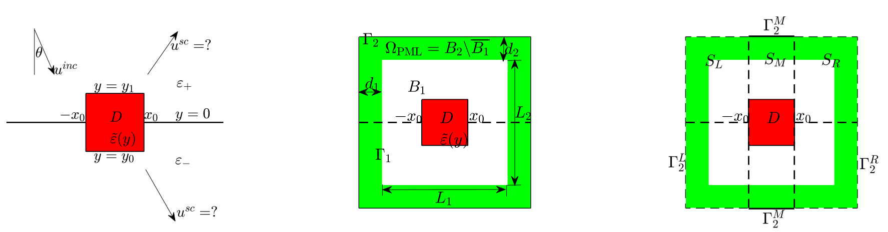

(a) (b) (c)

FIG. 1. (a) *A schematic of the scattering problem.* (b) *Using a PML to truncate* $\mathbb{R}^2$. (c) *Separated by* $x = \pm x_0$, *the truncated region is segmented into three segments* S_L *(left),* S_M *(middle), and* S_R *(right), while* $\Gamma_2 = \partial B_2$ *is divided into* Γ_2^L *(left dashed),* Γ_2^M *(middle solid), and* Γ_2^R *(right dashed). The shaded region* $\Omega_{\rm PML} = B_2 \backslash \overline{B_1}$ *indicates the PML region;* B_1 *consists of the whole white region and* $\bar{D}$*, and* B_2 *consists of the PML region* $\Omega_{\rm PML}$*,* B_1*, and* $\Gamma_1 = \partial B_1$.

where $\Delta = \partial_x^2 + \partial_y^2$ and k_0 is the free-space wavenumber. Across the interfaces $I = \partial D \cup \{(x,0) : |x| > x_0\}$, we have the following transmission condition:

$$[u^{\text{tot}}]_I = 0, \quad \left[\frac{\partial u^{\text{tot}}}{\partial \boldsymbol{\nu}}\right]_I = 0, \tag{3}$$

where $\boldsymbol{\nu}$ denotes the unit normal vector of a point on I, pointing towards $\mathbb{R}^2_-$ if the point is on $y = 0$ or pointing towards the exterior of D if the point is on ∂D, and $[\cdot]_I$ denotes the jump of the quantity across I. For electromagnetic waves in the E polarization, u^{tot} is the z component (the only nonzero component) of the electric field.

At infinity, the scattered wave field

$$u^{\text{sc}} = \begin{cases} u^{\text{tot}} - u^{\text{inc}}, & \text{in } \mathbb{R}^2_+\backslash\bar{D}; \\ u^{\text{tot}}, & \text{otherwise}, \end{cases}$$

in general is not outgoing, since u^{tot} involves the following reference field:

$$u^{\text{tot}}_{\text{ref}} = \begin{cases} e^{i(k_\rightarrow x - k_\uparrow y)} + Re^{i(k_\rightarrow x + k_\uparrow y)}, & (x,y) \in \mathbb{R}^2_+, \\ Te^{i(k_\rightarrow x - k_\downarrow y)}, & (x,y) \in \mathbb{R}^2_-, \end{cases} \tag{4}$$

which is the total field for the same incident wave scattering in the background two-layer medium but with no inhomogeneities. In (4), we obtain from Snell's law that

$$k_\downarrow = \sqrt{k_0^2 \varepsilon_- - k_\rightarrow^2}, \quad R = \frac{k_\uparrow - k_\downarrow}{k_\uparrow + k_\downarrow}, \quad T = R + 1. \tag{5}$$

Thus, subtracting from u^{tot} this reference field $u^{\text{tot}}_{\text{ref}}$ yields the following outgoing wave field:

$$u^{\text{og}} = \begin{cases} u^{\text{tot}} - u^{\text{tot}}_{\text{ref}}, & \text{in } \mathbb{R}^2\backslash\bar{D}; \\ u^{\text{tot}}, & \text{in } \ D. \end{cases}$$

More precisely, u^{og} should satisfy the following the half-plane Sommerfeld radiation condition in both $\mathbb{R}^2_+$ and $\mathbb{R}^2_-$, i.e.,

$$\lim_{r\to\infty} \sqrt{r}(\partial_r u^{\text{og}} - ik_0 n_\pm u^{\text{og}}) = 0, \quad r = \sqrt{x^2+y^2}. \tag{6}$$

Based on (6), we have the following existence and uniqueness results due to [25, 8, 1].

THEOREM 2.1. *For any incident plane wave with $k_0 > 0$, the scattering problem* (2) *and* (3) *has a unique solution u^{tot} in $H^1_{\text{loc}}(\mathbb{R}^2)$ provided that u^{og} satisfies* (6).

Since u^{og} is outgoing, the PML technique [2] is applicable to absorb u^{og}. Let us define the following complex coordinate stretching functions:

$$\tilde{x}(x) = x + i\int_0^x \sigma_1(t)dt, \quad \tilde{y}(y) = y + i\int_0^y \sigma_2(t)dt, \tag{7}$$

where $\sigma_l(t) = \sigma_l(-t)$ for all t, $\sigma_l(t) = 0$ for $|t| \le L_l/2$, and $\sigma_l(t) > 0$ for $|t| > L_l/2$, and $L_l > 0$ for $l = 1$, 2. As shown in Figure 1(b), rectangle $B_1 = (-L_1/2, L_1/2) \times (-L_2/2, L_2/2)$ encloses the inhomogeneity D, and rectangle $B_2 = (-L_1/2 - d_1, L_1/2 + d_1) \times (-L_2/2 - d_2, L_2/2 + d_2)$ is used to truncate $\mathbb{R}^2$, where domain $\Omega_{\text{PML}} = B_2\backslash\overline{B_1}$ with nonzero σ_l is the PML, and d_1 and d_2 denote thickness of the PML in x

and y directions, respectively. In the following, unless otherwise specified, we assume that $d_1 = d_2 = d$, and $\sigma_l \equiv \sigma$ when $|t| \geq L_l/2, l = 1, 2$ for some constants $d, \sigma > 0$.

By Green's representation theorem, we can define $u^{\rm og}(\tilde{\boldsymbol{r}}) = \mathbb{E}[u^{\rm og}](\boldsymbol{r})$ for $\boldsymbol{r} \in \Omega_{\rm PML}$ by

$$\mathbb{E}[g](\boldsymbol{r}) := \int_{\Gamma_1} [-G(\tilde{\boldsymbol{r}}; \boldsymbol{r}')\partial_{\boldsymbol{\nu}} g(\boldsymbol{r}') + \partial_{\boldsymbol{\nu}(\boldsymbol{r}')} G(\tilde{\boldsymbol{r}}; \boldsymbol{r}') g(\boldsymbol{r}')] ds(\boldsymbol{r}') \quad \forall g \in H^{1/2}(\Gamma_1), \tag{8}$$

where $\Gamma_1 = \partial B_1$, $\boldsymbol{r}' = (x', y')$, $\boldsymbol{r} = (x, y)$, $\tilde{\boldsymbol{r}} = (\tilde{x}, \tilde{y})$, and G denotes the layered medium Green's function; see [8, equations (4.2)–(4.5)]. Denoting $\tilde{u}^{\rm og}(\boldsymbol{r}) = u^{\rm og}(\tilde{\boldsymbol{r}})$, we see $\tilde{u}^{\rm og}$ satisfies the following PML-Helmholtz equation:

$$\nabla \cdot (A \nabla \tilde{u}^{\rm og}) + \alpha_1(x)\alpha_2(y) k_0^2 \varepsilon(x, y) \tilde{u}^{\rm og} = 0, \tag{9}$$

$$\tilde{u}^{\rm og}(x, 0+) = \tilde{u}^{\rm og}(x, 0-), \quad \partial_{\tilde{y}} \tilde{u}^{\rm og}(x, 0+) = \partial_{\tilde{y}} \tilde{u}^{\rm og}(x, 0-) \text{ in } \mathbb{R} \backslash [-x_0, x_0], \tag{10}$$

$$\tilde{u}^{\rm og}|_{\partial D}^{+} - \tilde{u}^{\rm og}|_{\partial D}^{-} = -u_{\rm ref}^{\rm tot}|_{\partial D}, \quad \partial_{\boldsymbol{\nu}} \tilde{u}^{\rm og}|_{\partial D}^{+} - \partial_{\boldsymbol{\nu}} \tilde{u}^{\rm og}|_{\partial D}^{-} = -\partial_{\boldsymbol{\nu}} u_{\rm ref}^{\rm tot}|_{\partial D}, \tag{11}$$

where $A = \text{diag}(\alpha_2(y)/\alpha_1(x), \alpha_1(x)/\alpha_2(y))$, $\alpha_l = 1 + i\sigma_l$, and $|_{\partial D}^{+}$ indicates the limit is taken from exterior of ∂D, etc.

Typically, a zero Dirichlet boundary condition is enforced on $\Gamma_2 = \partial B_2$, i.e.,

$$\tilde{u}^{\rm og}(x, y) = 0 \quad \text{on} \quad \Gamma_2. \tag{12}$$

Based on (12), we shall see in section 4 that $\tilde{u}^{\rm og}$ converges to $u^{\rm og}$ exponentially in the physical domain B_1. Consequently, we only need to deal with $\tilde{u}^{\rm og}$ in the bounded domain B_2 instead of $u^{\rm og}$ in $\mathbb{R}^2$.

3. NMM method.

For the scattering problem formulated above, the NMM methods are applicable, since, as shown in Figure 1(b) and (c), the structure, after the PML truncation, is uniform in x in three different segments: $S_L = \{(x, y) : -d_1 - L_1/2 < x < -x_0\} \cap B_2$, $S_M = \{(x, y) : |x| < x_0\} \cap B_2$, and $S_R = \{(x, y) : x_0 < x < d_1 + L_1/2\} \cap B_2$. Accordingly, $\Gamma_2 = \partial B_2$ is divided into the following three parts:

$$\Gamma_2^L = \{(x, y) \in \Gamma_2 : x < -x_0\},$$
$$\Gamma_2^M = \{(x, d_2 + L_2/2) : |x| < x_0\} \cup \{(x, -d_2 - L_2/2) : |x| < x_0\},$$
$$\Gamma_2^R = \{(x, y) \in \Gamma_2 : x > x_0\}.$$

In the last several decades, many different NMM methods have been developed. These methods use different numerical approaches to solve the eigenmodes in each uniform segment and also use different techniques to impose the continuity conditions at the interfaces between the neighboring segments. Our NMM method is similar to the one presented in [22], and its basic steps are summarized below.

We consider segments S_L and S_R first. According to (9)–(12), $\tilde{u}^{\rm og}$ in S_L and S_R solves

$$\nabla \cdot (A \nabla \tilde{u}^{\rm og}) + k_0^2 \alpha_1(x)\alpha_2(y) \varepsilon_{\pm}(y) \tilde{u}^{\rm og} = 0, \quad \pm y > 0, \tag{13}$$

$$\tilde{u}^{\rm og}(x, 0+) = \tilde{u}^{\rm og}(x, 0-), \quad \partial_{\tilde{y}} \tilde{u}^{\rm og}(x, 0+) = \partial_{\tilde{y}} \tilde{u}^{s}(x, 0-), \tag{14}$$

$$\tilde{u}^{\rm og}(x, d_2 + L_2/2) = \tilde{u}^{\rm og}(x, -d_2 - L_2/2) = 0 \tag{15}$$

and meets the following zero boundary conditions:

$$\tilde{u}^{\rm og}(-d_1 - L_1/2, y) = \tilde{u}^{\rm og}(d_1 + L_1/2, y) = 0. \tag{16}$$

By the method of separation of variables, inserting $\tilde{u}^{\rm og}(x,y) = \phi^{(m)}(y)\psi^{(m)}(x)$ into (13–16) for $S_m, m \in \{L, R\}$, we see that $\phi^{(L)}$ and $\phi^{(R)}$ satisfy the eigenvalue problem

$$\frac{1}{\alpha_2}\frac{d}{dy}\left(\frac{1}{\alpha_2}\frac{d\phi}{dy}\right) + k_0^2\varepsilon_\pm(y)\phi(y) = \delta\phi, \quad \pm y > 0, \tag{17}$$

$$\phi(0+) = \phi(0-), \phi'(0+) = \phi'(0-), \tag{18}$$

$$\phi(d_2 + L_2/2) = \phi(-d_2 - L_2/2) = 0 \tag{19}$$

and that $\psi^{(m)}(x)$ satisfies

$$\frac{1}{\alpha_1}\frac{d}{dx}\left(\frac{1}{\alpha_1}\frac{d\psi^{(m)}}{dx}\right) + \delta\psi^{(m)} = 0 \tag{20}$$

with the following boundary conditions:

$$\psi^{(L)}(-d_1 - L_1/2) = 0, \quad \psi^{(R)}(d_1 + L_1/2) = 0. \tag{21}$$

As in [29], we employ a pseudospectral method to find the eigenmodes. Assuming N eigenpairs $\{\delta_j, \phi_j(y)\}$ for $j = 1, \ldots, N$ are obtained based on the N collocation points $\{y^j\}_{j=1}^N \subset [-d_2 - L_2/2, d_2 + L_2/2]$, we can easily get the associated function $\psi_j^{(m)}$ from (20) and approximate $\tilde{u}^{\rm og}$ by

$$\tilde{u}^{\rm og} \approx \sum_{j=1}^N \left[l_j^{(L)} e^{-i\sqrt{\delta_j}(\tilde{x}(x) - \tilde{x}(-x_0))} + r_j^{(L)} e^{i\sqrt{\delta_j}(\tilde{x}(x) - \tilde{x}(-d_1 - L_1/2))}\right]\phi_j(y) \tag{22}$$

in S_L and by

$$\tilde{u}^{\rm og} \approx \sum_{j=1}^N \left[l_j^{(R)} e^{-i\sqrt{\delta_j}(\tilde{x}(x) - \tilde{x}(d_1 + L_1/2))} + r_j^{(R)} e^{i\sqrt{\delta_j}(\tilde{x}(x) - \tilde{x}(x_0))}\right]\phi_j(y) \tag{23}$$

in S_R, where $\sqrt{\delta_j}$ is defined to be in the branch with $\mathrm{Im}(\sqrt{\delta_j}) \geq 0$ and hence with $\mathrm{Re}(\sqrt{\delta_j}) \geq 0$ according to part (1) of Proposition A.1, and $r_j^{(m)}$ and $l_j^{(m)}$ are unknown coefficients of right-going and left-going eigenmodes in segment $S^{(m)}$, respectively, for $m \in \{L, R\}$. Based on the zero boundary condition (21), we get

$$r_j^{(L)} = -l_j^{(L)} e^{-i\sqrt{\delta_j}(\tilde{x}(-d_1 - L_1/2) - \tilde{x}(-x_0))}, \tag{24}$$

$$l_j^{(R)} = -r_j^{(R)} e^{i\sqrt{\delta_j}(\tilde{x}(d_1 + L_1/2) - \tilde{x}(-x_0))}. \tag{25}$$

According to part (2) of Proposition A.1,

$$|r_j^{(L)}| \leq |l_j^{(L)}| e^{-\mathrm{Im}(\sqrt{\delta_j})d_1 - \mathrm{Re}(\sqrt{\delta_j})\bar{\sigma}} \approx 0,$$
$$|l_j^{(R)}| \leq |r_j^{(R)}| e^{-\mathrm{Im}(\sqrt{\delta_j})d_1 - \mathrm{Re}(\sqrt{\delta_j})\bar{\sigma}} \approx 0$$

for sufficiently large $\bar{\sigma} = \sigma d$. Consequently, we can assume that there are no terms with coefficients $r_j^{(L)}$ and $l_j^{(R)}$ in (22) and (23), respectively. Physically, this corresponds to the fact that $u^{\rm og}$ should not contain incoming waves in the two exterior segments.

In segment S_M, we denote

$$\varepsilon_M(y) = \begin{cases} \varepsilon_+, & y > y_1, \\ \varepsilon_D(y), & y_0 < y < y_1, \\ \varepsilon_-, & y < y_0. \end{cases} \tag{26}$$

The method of separation of variables is not applicable to $\tilde{u}^{\mathrm{og}}$, since from (11) it doesn't satisfy the homogeneous transmission conditions (3) at $y = y_0$ and $y = y_1$. To resolve this issue, we consider $u_M^{\mathrm{og}} = u^{\mathrm{tot}} - u_{\mathrm{ref,M}}^{\mathrm{tot}}$, where the reference field $u_{\mathrm{ref,M}}^{\mathrm{tot}}$ solves the scattering problem for the same incident wave and for the above layered profile (26) extending to $\mathbb{R}^2$. We let $u_{\mathrm{ref,M}}^{\mathrm{tot}}$ be the solution with the same x-dependence as the incident wave. More details are given Proposition A.2.

Clearly, both $u_M^{\mathrm{og}} = u^{\mathrm{tot}} - u_{\mathrm{ref,M}}^{\mathrm{tot}}$ and its normal derivative on $y = y_0$ and $y = y_1$ are continuous. Then, we enforce the same zero Dirichlet boundary condition

$$\tilde{u}_M^{\mathrm{og}} = 0 \quad \text{on } \Gamma_2^M, \tag{27}$$

where $\tilde{u}_M^{\mathrm{og}}(x, y) = u_M^{\mathrm{og}}(\tilde{x}(x), \tilde{y}(y))$. The method of separation of variables can be applied to $\tilde{u}_M^{\mathrm{og}}$ now. Based on the same discretization points $\{y^j\}_{j=1}^N$, we obtain N eigenpairs $\{\delta_j^{(M)}, \phi_j^{(M)}(y)\}_{j=1}^N$ in S_M; then

$$\tilde{u}_M^{\mathrm{og}} \approx \sum_{j=1}^{N} \left[l_j^{(M)} e^{-i\sqrt{\delta_j^{(M)}}(x-x_0)} + r_j^{(M)} e^{i\sqrt{\delta_j^{(M)}}(x+x_0)} \right] \phi_j^{(M)}(y), \tag{28}$$

where $l_j^{(M)}$ and $r_j^{(M)}$ are unknown coefficients of the eigenmodes in S_M.

On the two interfaces between S_M and the other two segments S_L and S_R, i.e, at $x = \pm x_0$, we have the transmission conditions

$$\tilde{u}^{\mathrm{og}}(\pm x_0, y) - \tilde{u}_M^{\mathrm{og}}(\pm x_0, y) = \tilde{f}(\pm x_0, y), \tag{29}$$

$$\partial_x \tilde{u}^{\mathrm{og}}(\pm x_0, y) - \partial_x \tilde{u}_M^{\mathrm{og}}(\pm x_0, y) = \tilde{g}(\pm x_0, y), \tag{30}$$

where $\tilde{f}(x, y) = f(x, \tilde{y}(y))$, $\tilde{g}(x, y) = g(x, \tilde{y}(y))$, and

$$f(x, y) = u_{\mathrm{ref,M}}^{\mathrm{tot}}(x, y) - u_{\mathrm{ref}}^{\mathrm{tot}}(x, y), \quad g(x, y) = \partial_x u_{\mathrm{ref,M}}^{\mathrm{tot}}(x, y) - \partial_x u_{\mathrm{ref}}^{\mathrm{tot}}(x, y).$$

Collocating (29) and (30) at $y = y^j$ for $j = 1, \ldots, N$, and using (22), (23), and (28), we obtain a linear system

$$\boldsymbol{A} \begin{bmatrix} \boldsymbol{l}^{(L)} \\ \boldsymbol{l}^{(M)} \\ \boldsymbol{r}^{(M)} \\ \boldsymbol{r}^{(R)} \end{bmatrix} = \boldsymbol{b}, \tag{31}$$

where $\boldsymbol{A}$ is a $4N \times 4N$ matrix, $\boldsymbol{b}$ is a $4N \times 1$ matrix, $\boldsymbol{l}^{(L)} = [l_1^{(L)}, \ldots, l_N^{(L)}]^T$, etc. Solving the above system, we get $\tilde{u}^{\mathrm{og}}$ in S_L and S_R, and $\tilde{u}_M^{\mathrm{og}}$ in S_M; thus u^{tot} can be found in the physical domain B_1.

In the above, the NMM method is only presented for the case of a single inhomogeneous segment in a two-media layered background. It is straightforward to extend the NMM method to structures with multiple inhomogeneous segments that are uniform along the same direction. The NMM method can also be used to study scattering problems in the H polarization (the only nonzero component of the magnetic field is its z component) and problems involving perfect electrical conductor or perfect magnetic conductor scatterers.

4. A Robin-type boundary condition. As we mentioned in the introduction, the NMM method based on the zero Dirichlet condition (27) usually works, but in some special circumstances, it exhibits a slow convergence and even a divergence, since $u_M^{\rm og}$ may not be strictly outgoing. It should be pointed out that there is no contradiction with the exponential convergence of $\tilde{u}^{\rm og}$ to $u^{\rm og}$, since the PML is designed for terminating $u^{\rm og}$, but the NMM method applies the PML to terminate $u_M^{\rm og}$ in the interior segment S_M.

In fact, it is easy to deduce that

$$u_M^{\rm og} = (R - R_M e^{-2ik_\uparrow y_1}) e^{i(k_\rightarrow x + k_\uparrow y)} + u^{\rm og} \quad \text{for } y > y_1, \tag{32}$$

$$u_M^{\rm og} = (T - T_M e^{ik_\downarrow y_0 - ik_\uparrow y_1}) e^{i(k_\rightarrow x - k_\downarrow y)} + u^{\rm og} \quad \text{for } y < y_0, \tag{33}$$

where R and R_M (T and T_M) are the reflection (transmission) coefficients in (4) and (81). Therefore, $u_M^{\rm og}$ can be decomposed as an outgoing wave field and an up-going plane wave with y-wavenumber $k_\uparrow$ for $y > y_1$ or a down-going plane wave with y-wavenumber $k_\downarrow$ for $y < y_0$. Consequently, only when $k_\uparrow$ and $k_\downarrow$ are sufficiently far away from zero does $u_M^{\rm og}$ attenuate in the PML. However, this is not true for the following two cases:

a. For grazing incidences with θ close to $\pm\pi/2$, $k_\uparrow$ is close to 0.
b. For $n_- < n_+$ and at the critical angles $\theta = \pm \arcsin(n_-/n_+)$ for the onset of total internal reflection, $k_\downarrow = 0$.

Notice that $\tilde{u}^{\rm og} \approx 0$ at the exterior boundary of the PML; therefore,

$$\tilde{u}_M^{\rm og} \approx (R - R_M e^{-2ik_\uparrow y_1}) e^{i(k_\rightarrow x + k_\uparrow \tilde{y})} \quad \text{on } y = d + L_2/2,$$
$$\tilde{u}_M^{\rm og} \approx (T - T_M e^{ik_\downarrow y_0 - ik_\uparrow y_1}) e^{i(k_\rightarrow x - k_\downarrow \tilde{y})} \quad \text{on } y = -d - L_2/2.$$

However, the NMM method is not compatible with the above inhomogeneous boundary conditions. To overcome this difficulty, the following result is needed.

PROPOSITION 4.1. *The two fields $u^{\rm og}$ and $u_M^{\rm og}$ satisfy*

$$\partial_y u_M^{\rm og} - ik_\uparrow u_M^{\rm og} = \partial_y u^{\rm og} - ik_\uparrow u^{\rm og} \quad \text{on } y = d + L_2/2, \tag{34}$$

$$\partial_y u_M^{\rm og} + ik_\downarrow u_M^{\rm og} = \partial_y u^{\rm og} + ik_\downarrow u^{\rm og} \quad \text{on } y = -d - L_2/2. \tag{35}$$

Correspondingly,

$$(A\nabla \tilde{u}_M^{\rm og}) \cdot \boldsymbol{\nu} - ik_\uparrow \tilde{u}_M^{\rm og} = (A\nabla \tilde{u}^{\rm og}) \cdot \boldsymbol{\nu} - ik_\uparrow \tilde{u}^{\rm og} \quad \text{on } y = d_2 + L_2/2, \tag{36}$$

$$(A\nabla \tilde{u}_M^{\rm og}) \cdot \boldsymbol{\nu} - ik_\downarrow \tilde{u}_M^{\rm og} = (A\nabla \tilde{u}^{\rm og}) \cdot \boldsymbol{\nu} - ik_\downarrow \tilde{u}^{\rm og} \quad \text{on } y = -d_2 - L_2/2, \tag{37}$$

where $\boldsymbol{\nu}$ denotes the unit upward (downward) normal vector on $y = d_2 + L_2/2$ ($y = -d_2 - L_2/2$).

Proof. The proof is straightforward. ∎

The above proposition suggests the following homogeneous Robin boundary condition on Γ_2^M:

$$\frac{1}{\alpha_2} \partial_y \tilde{u}_M^{\rm og} - ik_\uparrow \tilde{u}_M^{\rm og} = (A\nabla \tilde{u}_M^{\rm og}) \cdot \boldsymbol{\nu} - ik_\uparrow \tilde{u}_M^{\rm og} = 0 \quad \text{on} \quad y = d_2 + L_2/2, \tag{38}$$

$$\frac{1}{\alpha_2} \partial_y \tilde{u}_M^{\rm og} + ik_\downarrow \tilde{u}_M^{\rm og} = -(A\nabla \tilde{u}_M^{\rm og}) \cdot \boldsymbol{\nu} + ik_\downarrow \tilde{u}_M^{\rm og} = 0 \quad \text{on} \quad y = -d_2 - L_2/2. \tag{39}$$

Based on the pseudospectral method [29] and the above boundary conditions, we can find the eigenmodes $\phi_j^{(M)}$ ($1 \le j \le N$), and expand $\tilde{u}_M^{\rm og}$ in S_M in these eigenmodes.

With this Robin boundary condition on Γ_2^M and the zero Dirichlet boundary condition on $\Gamma_2\backslash\overline{\Gamma_2^M}$, we can establish the following convergence theorem.

THEOREM 4.1. *Let $\bar\sigma = \sigma d$ such that $\gamma_0\bar\sigma \geq \max(k_{\min}^{-1}, d)$, where*

$$\gamma_0 = d/\sqrt{(L_1+d)^2+(L_2+d)^2}.$$

We have that for sufficiently large $\bar\sigma$, the PML problem (9)–(11) *equipped with the hybrid Dirichlet–Robin boundary condition*

$$\begin{cases} \tilde u^{\rm og} = 0 & \text{on} \quad \Gamma_2\backslash\overline{\Gamma}, \\ (A\nabla\tilde u^{\rm og})\cdot\boldsymbol{\nu} = iW\tilde u^{\rm og} & \text{on} \quad \Gamma, \end{cases} \tag{40}$$

has a unique solution $\tilde u^{\rm og}$ in $H^1(B_2)$, where W is piecewise smooth on Γ with $\mathrm{Re}(W)\geq 0$ *and* $\mathrm{Im}(W)\geq 0$, *$\Gamma\subset\Gamma_2$ is an open bounded set, and the unit normal vector $\boldsymbol{\nu}$ on Γ points outwards. Moreover, there exists a constant C, which depends only on $||W||_{L^\infty(\Gamma)}$, γ_0, $k_{\max}/k_{\min}$, and L_2/L_1, but independent of n_-, n_+, L_1, L_2, and d, such that*

$$\begin{aligned} ||u^{\rm og}-\tilde u^{\rm og}||_{H^1(B_1)} \leq{}& C(1+\hat C^{-1})\gamma_1(1+k_{\min}L_1)^3\alpha_m^3 \\ & (1+\bar\sigma/L_1)^2 e^{-k_{\min}\gamma_0\bar\sigma}||\tilde u^{\rm og}||_{H^{1/2}(\Gamma_1)}, \end{aligned} \tag{41}$$

where $k_{\min}=k_0\min(n_-,n_+)$, $k_{\max}=k_0\max(n_-,n_+)$, $\gamma_1 = e^{L_2\sqrt{|k_{\max}^2-k_{\min}^2|/2}}$, $\alpha_m = \sqrt{1+\sigma^2}$, and $\hat C = \frac{\min(1,\sigma^3)}{2(1+\sigma^2)^2\max(1,k_{\max}^2d^2)}$.

Remark 4.1. The configuration of our PML problem is quite similar to [8] except that in [8], D is impenetrable and zero Dirichlet boundary condition is used. Thus, the proof of this theorem could be quite similar. Some significant changes due to the above difference are the following: since D is penetrable now, the equivalent sesquilinear form to our PML problem is different from [8]; since hybrid Robin–Dirichlet boundary condition is equipped, the well-posedness of the PML problem in the PML domain $\Omega_{\rm PML}$ should be proved again. The rest is routine by following [8].

Proof of Theorem 4.1.[1] Let $u = u^{\rm og} - \chi_D u_{\rm ref}^{tot}$, where $\chi_D = 1$ in D and is zero elsewhere. Then, u satisfies

$$\Delta u + k^2 u = F, \tag{42}$$
$$[u]_I = 0, \quad [u]_I = 0. \tag{43}$$
$$\lim_{r\to\infty}\sqrt{r}(\partial_r u - ik_0 n_\pm u) = 0, \tag{44}$$

while $\tilde u = \tilde u^{\rm og} - \chi_D u_{\rm ref}^{tot}$ satisfies

$$\nabla\cdot(A\nabla\tilde u) + \alpha_1(x)\alpha_2(y)k^2\tilde u = F, \tag{45}$$
$$[\tilde u]_{I\cap B_2} = 0, \quad [A\nabla\tilde u\cdot\boldsymbol{\nu}]_{I\cap B_2} = 0, \tag{46}$$
$$\tilde u = 0 \quad \text{on} \quad \Gamma_2\backslash\bar\Gamma, \quad A\nabla\tilde u\cdot\boldsymbol{\nu} = iW\tilde u \quad \text{on} \quad \Gamma, \tag{47}$$

[1]Part of this proof is based on a personal communication with Prof. Weiying Zheng (zwy@lsec.cc.ac.cn).

where $k(x,y) = k_0\sqrt{\varepsilon(x,y)}$, and

$$F = \begin{cases} (\varepsilon_+ - \varepsilon_D(y))u_{\rm ref}^{\rm tot}, & (x,y) \in D\cap\mathbb{R}^2_+; \\ (\varepsilon_- - \varepsilon_D(y))u_{\rm ref}^{\rm tot}, & (x,y) \in D\cap\mathbb{R}^2_-; \\ 0, & \text{otherwise} \end{cases} \tag{48}$$

is supported in D. Let $a : H^1(B_1)\times H^1(B_1) \to \mathbb{C}$ be the sesquilinear form

$$a(\phi,\psi) = \int_{B_1} (\nabla\phi\cdot\nabla\bar{\psi} - k^2\phi\bar{\psi})dxdy - < T\phi,\psi >_{\Gamma_1}, \tag{49}$$

where $<\cdot,\cdot>$ stands for the inner product on $L^2(\Gamma_1)$ or the duality pairing between $H^{-1/2}(\Gamma_1)$ and $H^{1/2}(\Gamma_1)$, and the operator $T : H^{1/2}(\Gamma_1) \to H^{-1/2}(\Gamma_1)$ maps $u|_{\Gamma_1}$ to its derivative $\partial_{\boldsymbol{\nu}} u|_{\Gamma_1}$; the existence of T has been illustrated by [8, Theorem 3.3]. Then, the problem (42–44) is equivalent to the following weak formulation: Find $u \in H^1(B_1)$ such that

$$a(u,\psi) = < F,\psi > \quad \forall\psi\in H^1(B_1). \tag{50}$$

The well-posedness Theorem 2.1 developed in [1] in fact leads to the inf-sup condition

$$\sup_{0\neq\psi\in H^1(B_1)} \frac{a(\phi,\psi)}{||\psi||_{H^1(\Omega_1)}} \geq C||\phi||_{H^1(B_1)} \quad \forall\phi\in H^1(B_1) \tag{51}$$

for some constant $C > 0$.

On the other hand, let $\tilde{a} : H^1(B_1)\times H^1(B_1)\to\mathbb{C}$ be the following sesquilinear form:

$$\tilde{a}(\phi,\psi) = \int_{B_1} (\nabla\phi\cdot\nabla\bar{\psi} - k^2\phi\bar{\psi})dxdy - < \tilde{T}\phi,\psi >_{\Gamma_1} . \tag{52}$$

Here, $\tilde{T} : H^{1/2}(\Gamma_1) \to H^{1/2}(\Gamma_1)$ maps ϕ, the solution of the following Dirichlet problem in the PML layer, to its normal derivative $\partial_{\boldsymbol{\nu}}\phi$ on Γ_1:

$$\nabla\cdot(A\nabla\phi) + \alpha_1\alpha_2 k^2\phi = 0 \quad \text{in} \quad \Omega_{\rm PML} = B_2\backslash\bar{B}_1, \tag{53}$$

$$[\phi]_{I\cap\Omega_{\rm PML}} = \left[\frac{\partial\phi}{\partial y}\right]_{I\cap\Omega_{\rm PML}} = 0, \tag{54}$$

$$\phi = 0 \text{ on } \Gamma_1, \quad \phi = q_1 \text{ on } \Gamma_2\backslash\bar{\Gamma}, \quad (A\nabla\phi)\cdot\boldsymbol{\nu} - iW\phi = q_2 \text{ on } \quad \Gamma, \tag{55}$$

where $q_1 \in H^{1/2}(\Gamma_2\backslash\bar{\Gamma})$ and $q_2 \in H^{-1/2}(\Gamma)$. To justify operator $\tilde{T}$ is well-defined, we rewrite the above problem into the following weak formulation: Find $\phi\in H^1(\Omega_{\rm PML})$ with $\phi = 0$ on Γ_1 and $\phi = q_1$ on $\Gamma_2\backslash\bar{\Gamma}$ such that

$$c(\phi,v) = \langle q_2, v\rangle|_\Gamma \quad \forall v\in H^1_{0/\Gamma}(\Omega_{\rm PML}), \tag{56}$$

where $H^1_{0\backslash\Gamma}(\Omega_{\rm PML}) := \{v\in H^1(\Omega_{\rm PML}) : v = 0 \text{ on } \Gamma_1\cup\Gamma_2\backslash\bar{\Gamma}\}$, and

$$c(\varphi,\psi) = \int_{\Omega_{\rm PML}} (A\nabla\varphi\cdot\nabla\bar{\psi} - \alpha_1\alpha_2 k^2\varphi\bar{\psi})dxdy - i\int_\Gamma W\varphi\bar{\psi}ds \quad \forall\varphi,\psi\in H^1_{0\backslash\Gamma}(\Omega_{\rm PML}).$$

Introducing the weighted H^1-norm

$$|||\varphi|||_{H^1(\Omega)} = \left(||\nabla\varphi||^2_{L^2(\Omega)} + ||k\varphi||^2_{L^2(\Omega)}\right)^{1/2}$$

and the following H^1 equivalent norm

$$||\varphi||_{*,\Omega_{\rm PML}} = \left(||A\nabla\varphi||^2_{L^2(\Omega_{\rm PML})} + ||k\alpha_1\alpha_2\varphi||^2_{L^2(\Omega_{\rm PML})}\right),$$

we claim that

$$\sup_{0\neq\psi\in H^1_{0\backslash\Gamma}(\Omega_{\rm PML})} \frac{|c(\phi,\psi)|}{||\psi||_{H^1(\Omega_{\rm PML})}} \geq \hat{C}||\phi||_{*,\Omega_{\rm PML}} \quad \forall\phi\in H^1_{0\backslash\Gamma}(\Omega_{\rm PML}). \tag{57}$$

The proof follows almost the same arguments as [8, Lemma 5.1] since the extra term W here contributes to $\mathrm{Re}[c(\phi,\phi)]$ a nonnegative term $\int_\Gamma \mathrm{Im}(W)|\phi|^2ds$, and to $\mathrm{Im}[c(\phi,\phi)]$ a nonpositive term $-\int_\Gamma \mathrm{Re}(W)|\phi|^2 ds$, from the assumption on W. This implies that (53)–(55) has a unique solution so that $\tilde{T}$ is well-defined. Consequently, problem (45)–(47) is equivalent to the following weak formulation: Find $\tilde{u}\in H^1(B_1)$ such that

$$\tilde{a}(\tilde{u},\psi) =< F,\psi > \quad \forall\psi\in H^1(B_1). \tag{58}$$

Next, we see that for any $h\in H^{1/2}(\Gamma_1)$, $Th-\tilde{T}h = \frac{\partial w}{\partial\boldsymbol{\nu}}|_{\Gamma_1}$ where w is the solution to (53)–(55) with $q_1=\mathbb{E}(h)$ and $q_2 = A\nabla\mathbb{E}(h)\cdot\boldsymbol{\nu} - iW\mathbb{E}(h)$. Let

$$\begin{aligned} X(h) := \{\zeta\in H^1(\Omega_{\rm PML}) : \zeta = 0 \text{ on } \Gamma_1, \zeta=\mathbb{E}(h) \text{ on } \Gamma_2\backslash\bar{\Gamma},\\ (A\nabla\zeta)\cdot\boldsymbol{\nu} - iW\zeta = (A\nabla_x\mathbb{E}(h))\cdot\boldsymbol{\nu} - iW\mathbb{E}(h) \text{ on } \Gamma\}. \end{aligned}$$

Analogous to [8, Lemma 5.2], we could show from the coercivity of sesquilinear form c, i.e., (57), that

$$||Th-\tilde{T}h||_{H^{-1/2}(\Gamma)} = ||\partial_{\boldsymbol{\nu}} w||_{H^{-1/2}(\Gamma)} \leq (1+\hat{C}^{-1})\inf_{\zeta\in X(h)} ||\zeta||_{*,\Omega_{\rm PML}}. \tag{59}$$

Following the proof of [8, Lemma 7.1], we have from the definition of $X(h)$ that

$$\begin{aligned} \inf_{\zeta\in X(h)} ||\zeta||_{*,\Omega_{\rm PML}} \leq C(1+k_{\min}L_1)\alpha_m^2(||\mathbb{E}(h)||_{H^{1/2}(\Gamma_2\backslash\bar{\Gamma})}\\ + ||(A\nabla_x\mathbb{E}(h))\cdot\boldsymbol{\nu} - iW\mathbb{E}(h)||_{H^{-1/2}}(\Gamma)). \end{aligned}$$

Since $\mathbb{E}(h)$ is piecewise smooth on Γ,

$$(A\nabla_x\mathbb{E}(h))\cdot\boldsymbol{\nu} - iW\mathbb{E}(h) \in L^2(\Gamma)\cap L^\infty(\Gamma),$$

so that

$$||(A\nabla\mathbb{E}(h))\cdot\boldsymbol{\nu} - iW\mathbb{E}(h)||_{H^{-1/2}(\Gamma)} \leq C||\mathbb{E}(h)||_{W^{1,\infty}(\Gamma)},$$

where C now depends on the norm $||W||_{L^\infty(\Gamma)}$. Consequently, we have from [8, Lemma 7.1] that

$$\inf_{\zeta\in X(h)} ||\zeta||_{*,\Omega_{\rm PML}} \leq C\gamma_1(1+k_{\min}L_1)^3\alpha_m^3\left(1+\frac{\bar{\sigma}}{L_1}\right)^2 e^{-k_{\min}\gamma_0\bar{\sigma}}||h||_{H^{1/2}(\Gamma_1)}. \tag{60}$$

Finally, from (59), (60), and the relation

$$a(u-\tilde{u},v) =< T\tilde{u}-\tilde{T}\tilde{u}, v> \quad \forall v\in H^1(B_1),$$

we immediately obtain (41) from the inf-sup condition (51), which completes the proof of Theorem 4.1 by using arguments analogous to [8, Theorem 7.2]. ∎

Choosing $\Gamma = \Gamma_2^M$, and defining

$$W(x,y) = \begin{cases} k_\uparrow & \text{on } y = d_2 + L_2/2; \\ k_\downarrow & \text{on } y = -d_2 - L_2/2, \end{cases}$$

in (40), we see from Theorem 4.1 that our hybrid Dirichlet–Robin boundary condition still gives a numerical solution $\tilde{u}^{\rm og}$ that exponentially converges to $u^{\rm og}$ in the physical domain B_1; when $\Gamma = \emptyset$, (40) reduces to the usual Dirichlet boundary condition (12).

Theorem 4.1 is established for PMLs with constant and equal σ_1 and σ_2. In practice, we may set $\sigma_1(x)$ and $\sigma_2(y)$ as continuous functions to increase flexibility. For example, we may choose

$$\sigma_l(t) = \sigma \left(\frac{t - L_l/2}{d_l} \right)^m \quad \text{in } L_l/2 < |t| < L_l/2 + d_l, \quad l = 1, 2, \tag{61}$$

for a positive constant σ and an integer $m \geq 0$, where $m = 0$ corresponds to the constant case.

5. Cylindrical incident waves. The NMM methods are typically implemented for plane incident waves. For other incident waves, such as point or line sources and Gaussian beams, the NMM methods may be used with a Fourier transform that rewrites the incident wave as a superposition of plane waves. This approach is not very efficient, since it is necessary to solve the problem for many different incident plane waves. Alternatively, we can try to find a reference solution for the given non-plane incident wave in each uniform segment. This task is nontrivial for the interior segment corresponding to the inhomogeneity. In the following, we present an efficient method for computing the reference solutions when the incident wave is a cylindrical wave generated by a line source.

The incident cylindrical wave is $u^{\rm inc} = \frac{i}{4} H_0^{(1)}(k_0 n_+ \rho(x,y))$ corresponding to a line source at $(x^*, y^*) \in \mathbb{R}_+^2 \backslash \bar{D}$, where $\rho(x,y) = \sqrt{(x-x^*)^2 + (y-y^*)^2}$. The governing Helmholtz equation becomes

$$\Delta u^{\rm tot} + k_0^2 \varepsilon(x,y) u^{\rm tot} = -\delta(x - x^*)\delta(y - y^*). \tag{62}$$

Considering the location of the source, we have the following three cases:

(a) If $|x^*| < x_0$, we set $u_{\rm ref}^{\rm tot} \equiv 0$ and find a nonzero $u_{\rm ref,M}^{\rm tot}$.

(b) If $|x^*| > x_0$ and $y^* > y_1$, we set $u_{\rm ref,M}^{\rm tot} \equiv 0$ and find a nonzero $u_{\rm ref}^{\rm tot}$.

(c) If $|x^*| = x_0$, then we have to find nonzero $u_{\rm ref}^{\rm tot}$ and $u_{\rm ref,M}^{\rm tot}$.

We consider the typical case (a), where $u_{\rm ref,M}^{\rm tot}$ must be computed in segment S_M. The NMM method requires $u_{\rm ref,M}^{\rm tot}$ and its x-derivative at $x = \pm x_0$ to evaluate $\tilde{f}$ and $\tilde{g}$ in (29) and (30).

Following the one-dimensional profile $\varepsilon_M(y)$ given in (26), $\mathbb{R}^2$ can be split into three layers $y < y_0$, $y_0 < y < y_1$, and $y > y_1$. The wave field

$$u_{\rm M}^{\rm og} = \begin{cases} u_{\rm ref,M}^{\rm tot} - u^{\rm inc} & \text{in } y > y_1, \\ u_{\rm ref,M}^{\rm tot} & \text{otherwise} \end{cases}$$

is outgoing as $y \to \pm\infty$. Using the same PML as before and applying the technique of separation of variables to $\tilde{u}_{\rm M}^{\rm og}$, we obtain the eigenvalue problem

$$\frac{1}{\alpha_1} \frac{d}{dx} \left(\frac{1}{\alpha_1} \frac{d\psi}{dx} \right) = \delta \psi, \tag{63}$$

$$\psi(-L_1/2 - d_1) = \psi(L_1/2 + d_1) = 0 \tag{64}$$

and its associated equation

$$\frac{1}{\alpha_2}\frac{d}{dy}\left(\frac{1}{\alpha_2}\frac{d\phi}{dy}\right)+(k_0^2\varepsilon_M(y)+\delta)\phi=0, \tag{65}$$

$$\phi(-L_2/2-d_2)=\phi(L_2/2+d_2)=0. \tag{66}$$

Different from the main step of the NMM method, the separation of variables here leads to an eigenvalue problem for ψ (a function of x), instead of ϕ which is not continuous at $y=y_1$.

The eigenvalue problem for ψ can be solved by a pseudospectral method as in [29]. If N' numerical eigenpairs $\{\delta_j,\psi_j(x)\}_{j=1}^{N'}$ are obtained corresponding to the collocation points $\{x_j\}_{j=1}^{N'}\subset[-L_1/2-d_1,L_1/2+d_1]$, we approximate $\tilde{u}_{\rm M}^{\rm og}$ by

$$\tilde{u}_{\rm M}^{\rm og}\approx\begin{cases}\sum_{j=1}^{N'}c_j^te^{i\sqrt{k_0^2\varepsilon_++\delta_j}(y-y_1)}\psi_j(x), & y>y_1,\\ \sum_{j=1}^{N'}\phi_j(y)\psi_j(x), & y_0\le y\le y_1,\\ \sum_{j=1}^{N'}c_j^be^{-i\sqrt{k_0^2\varepsilon_-+\delta_j}(y-y_0)}\psi_j(x), & y<y_0,\end{cases} \tag{67}$$

where the square roots have nonnegative imaginary parts. Notice that only outgoing waves are retained in the top and bottom layers.

The functions $\phi_j(y)$ satisfy

$$\frac{d^2\phi_j}{dy^2}+(k_0^2\varepsilon_D(y)+\delta_j)\phi_j=0. \tag{68}$$

Since $\tilde{u}_{\rm M}^{\rm og}$ satisfies the transmission condition at $y=y_0$, we have

$$\phi_j(y_0)=c_j^b,\quad \phi_j'(y_0+)=-c_j^bi\sqrt{k_0^2\varepsilon_-+\delta_j}.$$

Therefore, we enforce the following Robin boundary condition:

$$\phi_j'(y_0+)=-i\sqrt{k_0^2\varepsilon_-+\delta_j}\phi_j(y_0). \tag{69}$$

At $y=y_1$, we can find the coefficients $\{c_j^{\rm ps},d_j^{\rm ps}\}_{j=1}^{N'}$ such that

$$\sum_{j=1}^{N'}c_j^{\rm ps}\psi_j(x)=\frac{i}{4}H_0^{(1)}(k_0n_+\rho(\tilde{x}(x),y_1)), \tag{70}$$

$$\sum_{j=1}^{N'}d_j^{\rm ps}\psi_j(x)=\frac{d}{dy}\frac{i}{4}H_0^{(1)}(k_0n_+\rho(\tilde{x}(x),y))|_{y=y_1} \tag{71}$$

are exactly satisfied at the collocation points $\{x_j\}_{j=1}^{N'}$. Since $u^{\rm tot}$ satisfies the transmission condition on $y=y_1$, we have

$$c_j^t+c_j^{\rm ps}=\phi_j(y_1),\quad ic_j^t\sqrt{k_0^2\varepsilon_++\delta_j}+d_j^{\rm ps}=\phi_j'(y_1-).$$

Eliminating c_j^t, the above yields the following Robin boundary condition:

$$\phi_j'(y_1-)-i\sqrt{k_0^2\varepsilon_++\delta_j}\phi_j(y_1)=d_j^{\rm ps}-i\sqrt{k_0^2\varepsilon_++\delta_j}c_j^{\rm ps}. \tag{72}$$

As shown in Proposition A.2, the boundary value problem (68), (69), and (72) has a unique solution. Using a pesudospectral method, we solve this boundary value problem and obtain $\phi_j(y)$ at the collocation points $\{y^j\}_{j=1}^{N}\cap[y_0,y_1]$. Finally, since $c_j^b=\phi_j(y_0)$ and $c_j^t=\phi_j(y_1)-c_j^{\rm ps}$, we have $\tilde{u}_{\rm M}^{\rm og}$ and $u_{\rm ref,M}^{\rm tot}$ in S_M. The other two cases (b) and (c) are similar; we omit the details here.

6. Numerical examples. In this section, we carry out several numerical experiments to exhibit the performance of our NMM method. In all examples, we take the physical domain $B_1 = (-2.5, 2.5) \times (-2.5, 2.5)$, the free-space wavenumber $k_0 = 2\pi/\lambda$ with wavelength $\lambda = 1.13$; in the PML, we choose $d_1 = d_2 = d$ and define $\sigma_1 = \sigma_2$ as in (61).

Example 1. In the first example, the background two-layer medium is separated by interface $y = 0$ with $\varepsilon(x, y) = 4$ in the top and $\varepsilon(x, y) = 1$ in the bottom. The inhomogeneity filled in domain $D = (-0.5, 0.5) \times (-1, 1)$ is the same as the medium in the top, so that the structure involves only two unbounded media separated by an interface, which is a local perturbation of the interface $y = 0$; see the dashed lines in Figure 2. The PML-BIE method recently developed in [21] is applicable to this problem and is used to validate our NMM method. Using 1000 points to discretize the interface in the PML-BIE method, we obtain a reference solution $u^{\rm sol}_{\rm REF}$. To quantify the accuracy of the NMM method, we define the following relative error:

$$e_{\rm rel} = \sqrt{\frac{\sum_{(x,y)\in S}(u^{\rm sol}_{\rm REF}(x,y) - u^{\rm sol}_{\rm NMM}(x,y))^2}{\sum_{(x,y)\in S}(u^{\rm sol}_{\rm REF}(x,y))^2}}. \tag{73}$$

Here, S consists of all grid points in the physical domain used in the NMM method, and $u^{\rm sol}_{\rm NMM}$ denotes our NMM solution; in the current example, the grid points in S are on the two vertical lines $x = 0.5$ and $x = -0.5$ with $y \in [-2.5, 2.5]$.

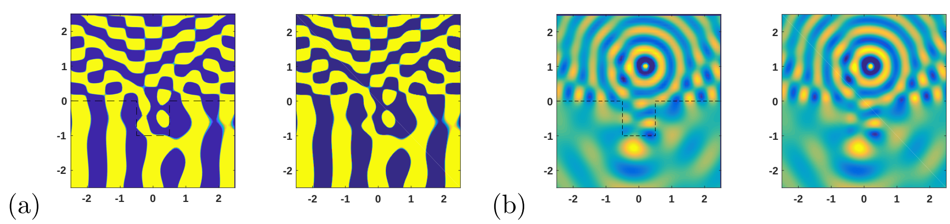

FIG. 2. *Example* 1*: Numerical solutions of a scattering problem in E polarization:* (a) *plane wave at critical incident angle $\theta = \pi/6$;* (b) *cylindrical wave for a source at* (0.2, 1)*. For both* (a) *and* (b)*, the reference solution by the PML-BIE method is shown on the left and the numerical solution by the NMM method is shown on the right.*

First, we validate the Robin-type boundary condition. We choose $\sigma = 70$, $d = 0.05$, and $m = 0$ to set up the PML. For both E and H polarizations, we choose $N = 950$ eigenmodes in each segment and compute $e_{\rm rel}$ for incident angle θ varying in $[0, \pi/2)$. The results are shown in Figure 3(a) and (b). It is clear that in the vicinity of the critical angle $\theta = \pi/6$, where total internal reflection first occurs, or $\theta = \pi/2$, which gives horizontally propagating incident plane waves, the Robin boundary condition produces a much smaller $e_{\rm rel}$ and significantly outperforms the Dirichlet boundary condition.

At both the critical incident angle $\theta = \pi/6$ and the normal incidence with $\theta = 0$, we study the relation between $e_{\rm rel}$ and the PML thickness d for a fixed $\sigma = 70$. The numerical results are shown in Figure 3(c) and (d), where both axes are scaled logarithmically. When d is small, we expect that the error is dominated by the truncation of the PML. The results in Figure 3(c) and (d) indicate that $e_{\rm rel}$ initially decays exponentially as d is increased, which numerically validates Theorem 4.1.

Finally, we compare the numerical solutions of the total field $u^{\rm tot}$ by the NMM and PML-BIE methods for two types of incident waves: a plane wave with the critical

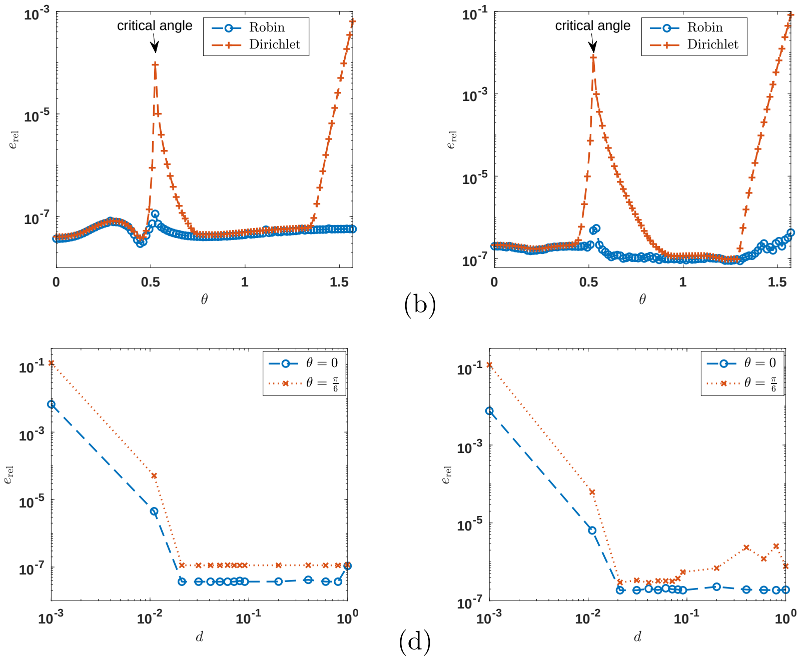

(a) (b) (c) (d)

FIG. 3. *Example* 1*:* (a) *and* (b)*: Relative error versus incident angle θ using Robin and Dirichlet boundary conditions on Γ_2^2 for $N = 950$, $\sigma = 70$, $d = 0.05$, and $m = 0$.* (c) *and* (d)*: Relative error versus PML thickness d at $\theta = 0$ and $\theta = \pi/6$ for $N = 950$, $m = 0$, and $\sigma = 70$.* (a, c) *E polarization;* (b, d) *H polarization.*

incident angle $\theta = \pi/6$, and a cylindrical wave excited by a source at $(0.2, 1)$. The results are shown in Figure 2. For each case, the PML-BIE solution is shown on the left and the NMM solution is shown on the right. Clearly, the solutions obtained by the two numerical methods are nearly indistinguishable from each other.

Example 2. The dielectric function $\varepsilon(x, y)$ is profiled by Figure 4(c), where $\varepsilon(x, y)$ is 4 in the top layer, 1 in the bottom layer, and $(1.5 - y)^2$ in the inhomogeneity $D = (-0.5, 0.5) \times (-0.5, 0.5)$.

Since $\varepsilon(x, y)$ is variable in D, the PML-BIE method is no longer applicable. We use the NMM method to find the total field $u^{\rm tot}$ for the E polarization and for two different incident waves: a plane wave at the critical incident angle $\theta = \pi/6$, and a cylindrical wave excited by a source at $(0.2, 1)$.

For these two incident waves, using $N = 1014$ eigenmodes in each segment and using $m = 1$, $\sigma = 70$, and $d = 1$ to set up the PML, we obtain two numerical solutions, relatively, as shown in Figure 4(a) and (b). Using the above two numerical solutions as reference solutions, relatively, we compute $e_{\rm rel}$ defined in (73) for numerical solutions with values of d less than 1, for the two incident waves, relatively; see Figure 4(d). As before, when d is small, the relative error decays exponentially, since it is dominated by the truncation of the PML.

Example 3. The dielectric function $\varepsilon(x, y)$ is profiled by Figure 5(c), where two inhomogeneities are embedded in the background medium with three layers. Here, $\varepsilon(x, y)$ is 4, 2.25, and 1 in the top, inner, and bottom layers, respectively. In the two inhomogeneities,

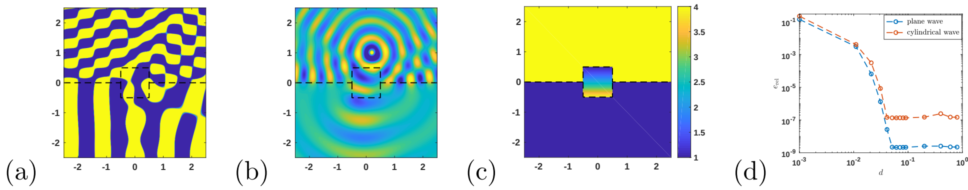

Fig. 4. *Example 2: Numerical solutions of a scattering problem in the E polarization:* (a) *plane wave at critical incident angle $\theta = \pi/6$;* (b) *cylindrical wave for a source at* $(0.2, 1)$*;* (c) *profile of the dielectric function $\varepsilon(x, y)$;* (d) *relative error e_{rel} versus PML thickness d. In* (a) *and* (b)*, we take $N = 1014$, $m = 1$, $\sigma = 70$, and $d = 1$.*

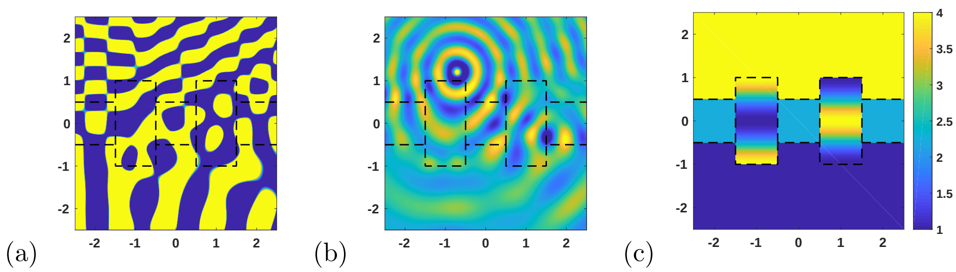

Fig. 5. *Example 3: Numerical solutions of a scattering problem in the E polarization:* (a) *plane wave at critical incident angle $\theta = \pi/6$;* (b) *cylindrical wave for a source at* $(-0.7, 1.2)$*;* (c) *profile of the dielectric function $\varepsilon(x, y)$. Other parameters: $N = 633$, $m = 0$, $\sigma = 70$, and $d = 1$.*

$$\varepsilon(x, y) = \begin{cases} (1 + \sin^2(\pi y/2))^2, & (x, y) \in D_1 = (-1.5, -0.5) \times (-1, 1); \\ (1 + \cos^2(\pi y/2))^2, & (x, y) \in D_2 = (0.5, 1.5) \times (-1, 1). \end{cases}$$

Using $N = 633$ eigenmodes in each segment, and using $m = 0$, $\sigma = 70$, and $d = 1$ to set up the PML, we calculate the total field u^{tot} for the E polarization and for two different incident waves: a plane wave with the critical incident angle $\theta = \pi/6$, and a cylindrical wave excited by a source at $(-0.7, 1.2)$. The results are shown in Figure 5(a) and (b).

7. Conclusion. The NMM methods are widely used in engineering applications for simulating propagation and scattering of linear electromagnetic, acoustic, and elastic waves. These methods are restricted to special structures but are more efficient than the standard numerical methods when they are applicable, since no discretization is needed for one spatial variable. In this paper, a new NMM method is developed to overcome a limitation of existing NMM methods due to the existence of a nonpropagating and nondecaying wave field component. A Robin-type boundary condition is used to ensure that the wave field component with zero or near-zero transverse wavenumber is not reflected by a truncated PML. A theoretical foundation of the new NMM is established by a theorem which reveals the exponential convergence of the PML solution with the hybrid Dirichlet–Robin boundary conditions. In addition, for scattering problems with cylindrical incident waves, we developed a fast method to compute reference solutions needed in the NMM methods. Numerical examples are presented to validate the NMM method and illustrate its performance.

We have implemented the new NMM method for two-dimensional structures with one or more inhomogeneities, for electromagnetic waves in E and H polarizations, and for both plane and cylindrical incident waves. The NMM methods are also applicable to three-dimensional (3D) rotationally symmetric structures that are piecewise uniform in the radial variable [15, 22]. There is also a related method for more general 3D structures without the rotational symmetry [28, 27]. The techniques developed in this paper, namely, the Robin-type boundary condition for terminating the PML and the fast method for computing reference solutions for cylindrical incident waves, should also be useful in these NMM and related methods for 3D structures.

Appendix A. Proof of Propositions.

PROPOSITION A.1. *Let*

$$\varepsilon_{\mathrm{gen}}(y) = \begin{cases} \varepsilon_+, & y > y_1, \\ \varepsilon_-, & y < y_0, \\ \varepsilon_{\mathrm{PHY}}(y), & y_0 \le y \le y_1, \end{cases}$$

where $\varepsilon_{\mathrm{PHY}}$ *is a piecewise constant and positive function. Then, the eigenvalue problem*

$$\frac{1}{1+i\sigma_2(y)}\frac{d}{dy}\left(\frac{1}{1+i\sigma_2(y)}\frac{d\phi}{dy}\right) + k_0^2\varepsilon_{\mathrm{gen}}(y)\phi(y) = \delta\phi, \quad |y| < d_2 + L_2/2, \tag{74}$$

$$\phi(y-) = \phi(y+), \phi'(y-) = \phi'(y+), \quad y \in \{y \in \mathbb{R} : \varepsilon_{\mathrm{gen}} \text{ is discontinuous at } y\}, \tag{75}$$

$$\phi(d_2 + L_2/2) = \phi(-d_2 - L_2/2) = 0, \tag{76}$$

where $d_2 = d$ *and* $\sigma_2(y) = \sigma$ *for* $|y| \ge L_2/2$ *for positive constants* d *and* σ*, satisfies the following:*

(1) *One and only one of the following two cases:*
   (a) *There exist* $\sigma^0 > 0$ *and* $d^0 > 0$ *such that if* $\sigma > \sigma^0$ *or if* $d > d^0$*, then* $\mathrm{Im}(\delta) \ge 0$ *for any eigenpair* $\{\phi, \delta\}$ *that solves* (17)–(19)*;*
   (b) *For a fixed* $d > 0$ $(\sigma > 0)$*, there exist a sequence of* $\{\sigma^n\}_{n=1}^{\infty}(\{d^n\}_{n=1}^{\infty}$*, respectively) that approaches infinity as* $n \to \infty$ *such that there exists a sequence of associated eigenpairs* $\{\phi^n, \delta^n\}$ *with* $||\phi^n||_{L^2(-L_2/2,L_2/2)} = 1$ *satisfying* $\mathrm{Im}(\delta^n) < 0$.

   If case (b) *holds, then* $\mathrm{Im}(\delta^n) \to 0$ *as* $n \to \infty$ *and*

$$\max(k_0^2\varepsilon_+, k_0^2\varepsilon_-) \le \liminf_{n\to\infty} \mathrm{Re}(\delta^n) \le \limsup_{n\to\infty} \mathrm{Re}(\delta^n) < \max(k_0^2\varepsilon_{\mathrm{gen}}).$$

(2) $\lim_{\bar\sigma\to\infty}(\mathrm{Im}(\sqrt{\delta}) + \mathrm{Re}(\sqrt{\delta})\sigma)d = +\infty$ *for any eigenpair* $\{\phi, \delta\}$*, where we recall that* $\bar\sigma = \sigma d$.

Proof. Part (1). It is clear that if case (a) does not hold, then case (b) must hold. We now prove $\mathrm{Im}(\delta^{\mathrm{n}}) \to 0$ as $n \to \infty$ in case (b). Integrating (17) with $\bar\phi$ on $[-L_2/2, L_2/2]$ and using integration by parts yields

$$\begin{aligned} \delta\int_{-L_2/2}^{L_2/2}|\phi^n|^2dy = &-\int_{-L_2/2}^{L_2/2}|\phi^{n,'}(y)|^2dy + k_0^2\int_{-L_2/2}^{L_2/2}\varepsilon_{\mathrm{gen}}|\phi^n|^2dy \\ &+ \left(\frac{d\phi^n}{dy}\bar{\phi^n}\right)\Big|_{-L_2/2}^{L_2/2}. \end{aligned} \tag{77}$$

In $\mathrm{PML}_y = (-L_2/2 - d, -L_2/2) \cup (L_2/2, L_2/2 + d)$, $\phi^n(y)$ has the following general solution form:

$$\phi^n(y) = c_\pm^{1,n}e^{\pm ik_\pm^{*,n}(\tilde y \mp L_2/2)} + c_\pm^{2,n}e^{\mp ik_\pm^{*,n}(\tilde y \mp L_2/2)} \quad \text{in } \mathrm{PML}_y \cap \mathbb{R}_\pm,$$

where $k_\pm^{*,n} = \sqrt{k_0^2\varepsilon_\pm - \delta^n}$ with $\mathrm{Re}(k_\pm^{*,n}) \ge 0$. Since $\mathrm{Im}(\delta^n) < 0$, $\mathrm{Im}(k_\pm^{*,n}) > 0$.

The homogeneous Dirichlet boundary condition at $y = \pm(L_2/2 + d)$ implies that

$$c_{\pm}^{2,n} = -c_{\pm}^{1,n} e^{2ik_{\pm}^{*,n} d^n (1+i\sigma^n)},$$

so that, by a straightforward calculation, one obtains

$$\left(\frac{d\phi^n}{dy}\bar{\phi}^n\right)\Big|_{-L_2/2}^{L_2/2} = \sum_{p=\pm} |c_p^{1,n}|^2 \Big[(1 - e^{-4d^n(\mathrm{Im}(k_p^{*,n})+\mathrm{Re}(k_p^{*,n})\sigma^n)}) i k_p^{*,n}$$

$$(78) \qquad -2k_p^{*,n} e^{-2d^n(\mathrm{Im}(k_p^{*,n})+\mathrm{Re}(k_p^{*,n})\sigma^n)} \sin(2d^n(\mathrm{Re}(k_p^{*,n}) - \mathrm{Im}(k_p^{*,n})\sigma^n))\Big].$$

Now, we assert $\lim_{n\to\infty} \mathrm{Re}(k_p^{*,n}) = 0$ holds for every $p \in \{+,-\}$. Suppose if there exists a subsequence $\{n_l\}$ such that $\lim_{l\to\infty} \mathrm{Re}(k_+^{*,n_l}) = K > 0$, then the imaginary parts of (78) and (77) indicate that $\lim_{l\to\infty} \mathrm{Im}(\delta^{n_l}) = 0$. But this leads to $\lim_{l\to\infty} \mathrm{Im}(k_+^{*,n_l}) = 0$ by $-\mathrm{Im}(\delta^{n_l}) = 2\mathrm{Im}(k_+^{*,n_l})\mathrm{Re}(k_+^{*,n_l})$. We claim $\liminf_{l\to\infty} |c_+^{1,n_l}| > 0$. Otherwise, we distinguish two cases: First, $K = +\infty$, so that $\lim_{l\to\infty} \mathrm{Re}(\delta^{n_l}) = -\infty$, and therefore

$$\liminf_{l\to\infty} |c_+^{1,n_l}| = 0, \quad \liminf_{l\to\infty} |c_+^{2,n_l}| = 0.$$

In the second case, $K < +\infty$, so that $\{k_+^{*,n_l}\}$ is a bounded sequence which indicates that

$$\liminf_{l\to\infty} |\phi^{n_l}(L_2/2)| = 0, \quad \liminf_{l\to\infty} |\phi^{n_l,'}(L_2/2)| = 0.$$

Using the general solution form of ϕ^{n_l} in each homogeneous region in $[-L_2/2, L_2/2]$, one could check in either of the above two cases that

$$\liminf_{l\to\infty} ||\phi^{n_l}||_{L^2(-L_2/2,L_2/2)} = 0,$$

which contradicts the assumption $||\phi^{n_l}||_{L^2(-L_2/2,L_2/2)} = 1$. But considering the imaginary part of (78) again, we obtain

$$\limsup_{l\to\infty} \mathrm{Im}\left(\frac{d\phi^{n_l}}{dy}\bar{\phi}^{n_l}\right)\Big|_{-L_2/2}^{L_2/2} > 0.$$

Consequently, $\limsup_{n\to\infty} \mathrm{Im}(\delta^n) > 0$ by (77) which is impossible.

Now considering the real parts of (78) and (77), we immediately get

$$\limsup_{n\to\infty} \mathrm{Re}(\delta^n) < k_0^2 \max(\varepsilon_{\mathrm{gen}}),$$

since $\varepsilon_{\mathrm{gen}}$ is nonconstant. On the other hand,

$$(79) \qquad \mathrm{Re}(\delta^n) = k_0^2\varepsilon_\pm - \mathrm{Re}(k_\pm^{*,n})^2 + \mathrm{Im}(k_\pm^{*,n})^2 \geq k_0^2\varepsilon_\pm - \mathrm{Re}(k_\pm^{*,n})^2,$$

so that

$$\liminf_{n\to\infty} \mathrm{Re}(\delta^n) \geq k_0^2\varepsilon_\pm, \quad \limsup_{n\to\infty} \mathrm{Im}(k_\pm^{*,n})^2 < k_0^2 \max(\varepsilon_{\mathrm{gen}}) - k_0^2\varepsilon_\pm.$$

Consequently, as $n \to \infty$, we have $\mathrm{Im}(\delta^n) = -2\mathrm{Im}(k_\pm^{*,n})\mathrm{Re}(k_\pm^{*,n}) \to 0$.

Part (2). Suppose there exist a sequence of $\{\bar{\sigma}^n = \sigma^n d^n\}$ that approaches infinity as $n \to \infty$ such that the associated eigenpairs $\{\phi^n, \delta^n\}$ with $||\phi^n||_{L^2(-L_2/2,L_2/2)} = 1$ satisfy

$$\lim_{n\to\infty}(\mathrm{Im}(\sqrt{\delta^n})+\mathrm{Re}(\sqrt{\delta^n})\sigma^n)d^n<+\infty; \tag{80}$$

then we conclude that there exist a subsequence $\{n_l\}$ such that $\lim_{l\to\infty}\mathrm{Im}(\delta^{n_l})=0$. Since, if $\liminf_{n\to\infty}\mathrm{Im}(\delta^n)>0$ (cannot be negative due to part (1) above), then we get $\lim_{n\to\infty}\mathrm{Re}(\sqrt{\delta^n})=0$ and $\limsup_{n\to\infty}\mathrm{Im}(\sqrt{\delta^n})<+\infty$, which implies

$$\lim_{n\to\infty}\mathrm{Im}(\delta^n)=\lim_{n\to\infty}2\mathrm{Im}(\sqrt{\delta^n})\mathrm{Re}(\sqrt{\delta^n})=0.$$

Besides, we have $\limsup_{l\to\infty}\mathrm{Re}(\delta^{n_l})\le 0$, since otherwise $\limsup_{l\to\infty}\mathrm{Re}(\sqrt{\delta^{n_l}})>0$ such that (80) cannot hold.

From (79), we get $\liminf_{l\to\infty}\mathrm{Re}(k_\pm^{*,n_l})\ge\sqrt{k_0^2\varepsilon_\pm}$. But this indicates again

$$\limsup_{l\to\infty}\mathrm{Im}\left(\frac{d\phi^{n_l}}{dy}\bar{\phi}^{n_l}\right)\Big|_{-L_2/2}^{L_2/2}\ge\liminf_{l\to\infty}|c_+^{1,n_l}|^2k_0\sqrt{\varepsilon_+}+|c_-^{1,n_l}|^2k_0\sqrt{\varepsilon_-}>0,$$

so that $\limsup_{l\to\infty}\mathrm{Im}(\delta^{n_l})>0$, which is a contradiction. ◻

Proposition A.2. *The field*

$$u_M^{\mathrm{tot}}=e^{-ik_\uparrow y_1}\begin{cases} e^{ik_\rightarrow x}(e^{-ik_\uparrow(y-y_1)}+R_Me^{ik_\uparrow(y-y_1)}) & \text{if } y\ge y_1,\\ e^{ik_\rightarrow x}q(y) & \text{if } y_0<y<y_1,\\ T_Me^{i(k_\rightarrow x-k_\downarrow(y-y_0))} & \text{if } y\le y_0.\end{cases} \tag{81}$$

solves the scattering problem (2) *and* (3) *with* $\varepsilon(x,y)=\varepsilon_M(y)$ *in* $\mathbb{R}^2$, *where* $k_\downarrow$ *was defined in* (5), *the unknown function* $q\in C^2[y_0,y_1]$ *is uniquely determined by the boundary value problem*

$$q''+(k_0^2\varepsilon_2-k_\rightarrow^2)q=0, \tag{82}$$
$$q'(y_0+)=-ik_\downarrow q(y_0), \tag{83}$$
$$q'(y_1-)=ik_\uparrow(q(y_1)-2), \tag{84}$$

and

$$R_M=q(y_1)-1,\quad T_M=q(y_0).$$

Proof. The verification that u_M^{tot} defined in (81) is indeed a solution is straightforward. One only needs to prove that the boundary value problem (82)–(84) has a unique solution. By the standard ODE theory, one needs to show that (82) with homogeneous Robin boundary conditions (replace 2 by 0 in (84)) has only the trivial solution $q=0$. To show this, integrating (82) with $\bar{q}$ on $[y_0,y_1]$ yields, by integration by parts,

$$\int_{y_0}^{y_1}q'\bar{f}'dy-(k_0^2\varepsilon_D-k_\rightarrow^2)q\bar{q}dy-(ik_\uparrow q(y_1)\bar{q}(y_1)+ik_\downarrow q(y_0)\bar{q}(y_0))=0.$$

Its imaginary part indicates

$$k_\uparrow|q(y_1)|^2+\mathrm{Re}(k_\downarrow)|q(y_0)|^2=0,$$

so that $q(y_1)=0$ since $k_\uparrow>0$. Then, $q'(y_1-)=ik_\uparrow q(y_1)=0$ indicates that $q\equiv 0$. ◻

Acknowledgments. The first author thanks Prof. Weiying Zheng from Institute of Computational Mathematics, Chinese Academy of Sciences, Prof. Haijun Wu from Nanjing University, and Prof. Guanghui Hu from Beijing Computational Science Research Center for some helpful discussions. We thank the two anonymous referees for their helpful suggestions.

REFERENCES

[1] G. Bao, G. Hu, and T. Yin, *Time-harmonic acoustic scattering from locally perturbed half-planes*, SIAM J. Appl. Math., 78 (2018), pp. 2672–2691.

[2] J.-P. Berenger, *A perfectly matched layer for the absorption of electromagnetic waves*, J. Comput. Phys., 114 (1994), pp. 185–200.

[3] P. Bienstman and R. Baets, *Optical modelling of photonic crystals and VCSELS using eigenmode expansion and perfectly matched layers*, Opt. Quantum Electron., 33 (2001), pp. 327–341.

[4] P. Bienstman, H. Derudder, R. Baets, F. Olyslager, and D. De Zutter, *Analysis of cylindrical waveguide discontinuities using vectorial eigenmodes and perfectly matched layers*, IEEE Trans. Microw. Theory Tech., 49 (2001), pp. 349–354.

[5] L. C. Botten, M. S. Craig, and R. C. McPhedran, *Highly conducting lamellar diffraction gratins*, Optica Acta, 28 (1981), pp. 1103–1106.

[6] O. P. Bruno, M. Lyon, C. Pérez-Arancibia, and C. Turc, *Windowed Green function method for layered-media scattering*, SIAM J. Appl. Math., 76 (2016), pp. 1871–1898.

[7] W. Cai, *Algorithmic issues for electromagnetic scattering in layered media: Green's functions, current basis, and fast solver*, Adv. Comput. Math., 16 (2002), pp. 157–174.

[8] Z. Chen and W. Zheng, *Convergence of the uniaxial perfectly matched layer method for time-harmonic scattering problems in two-layered media*. SIAM J. Numer. Anal., 48 (2010), pp. 2158–2185.

[9] W. C. Chew, *Waves and Fields in Inhomogeneous Media*, IEEE Press, New York, 1995.

[10] Y.-P. Chiou, W.-L. Yeh, and N.-Y. Shih, *Analysis of highly conducting lamellar gratings with multidomain pseudospectral method*, J. Lightwave Technol., 27 (2009), pp. 5151–5159.

[11] H. Derudder, De Zutter D., and F. Olyslager *Analysis of waveguide discontinuities using perfectly matched layers*, Electron. Lett., 34 (1998), pp. 2138–2140.

[12] G. Granet, *Reformulation of the lamellar grating problem through the concept of adaptive spatial resolution* J. Opt. Soc. Am. A, 16 (1999), pp. 2510–2516.

[13] G. Granet and B. Guizal, *Efficient implementation of the coupled-wave method for mettalic lamellar gratings in TM polarization*, J. Opt. Soc. Am. A, 13 (1996), pp. 1019–1023.

[14] P. Ho and Y. Y. Lu *A mode preserving perfectly matched layer for optical waveguides*, IEEE Photon. Tech. Lett., 15 (2003), pp. 1234–1236.

[15] Z. Hu, J. Lin, Y. Y. Lu, and S.-H. Oh, *Fast vertical mode expansion method for the simulation of extraordinary terahertz field enhancement in an annular nanogap*, J. Opt. Soc. Am. B, 35 (2018), pp. 30–38.

[16] K. Knop, *Rigorous diffraction theory for transmission phase gratings with deep rectangular grooves*, J. Opt. Soc. Am., 68 (1978), pp. 1206–1210.

[17] J. Lai, L. Greengard, and M. OŃeil, *A new hybrid integral representation for frequency domain scattering in layered media*, Appl. Comput. Harmon. Anal., 45 (2018), pp. 359–378.

[18] P. Lalane and G. M. Morris, *Highly improved convergence of the coupled-wave method for tm polarization*, J. Opt. Soc. Am. A, 13 (1996), pp. 779–784.

[19] L. Li, *A modal analysis of lamellar diffraction gratings in conical mountings*, J. Modern Opt., 40 (1993), pp. 553–573.

[20] L. Li, *Use of fourier series in the analysis of discontinuous periodic structures*, J. Opt. Soc. Am. A, 13 (1996), pp. 1870–1876.

[21] W. Lu, Y. Y. Lu, and J. Qian, *Perfectly matched layer boundary integral equation method for wave scattering in a layered medium* SIAM J. Appl. Math., 78 (2018), pp. 246–265.

[22] X. Lu, H. Shi, and Y. Y. Lu, *Vertical mode expansion method for transmission of light through a circular hole in a slab*, J. Opt. Soc. Am. A, 31 (2014), pp. 293–300.

[23] P. Monk, *Finite Element Methods for Maxwell's Equations*, Oxford University Press, Oxford, UK, 2003.

[24] R. H. Morf, *Exponentially convergent and numerically efficient solution of Maxwell's equations for lamellar gratings*, J. Opt. Soc. Am. A, 12 (1995), pp. 1043–1056.

[25] G. F. Roach and B. Zhang *The limiting-amplitude principle for the wave propagation problem with two unbounded media*, Math. Proc. Cambridge Philos. Soc., 112 (1992), pp. 207–223.

[26] P. Sheng, R. S. Stepleman, and P. N. Sanda, *Exact eigenfunctions for square wave gratings – application to diffraction and surface-plasmon calculations*, Phys. Rev. B, 26 (1982), pp. 2907–2916.

[27] H. Shi, X. Lu, and Y. Y. Lu, *Vertical mode expansion method for numerical modeling of biperiodic structures*, J. Opt. Soc. Am. A, 33 (2016), pp. 836–844.

[28] H. Shi and Y. Y. Lu, *Efficient vertical mode expansion method for scattering by arbitrary layered cylindrical structures*, Opt. Expr., 23 (2015), pp. 14618–14629.

[29] D. Song, L. Yuan, and Y. Y. Lu, *Fourier-matching pseudospectral modal method for diffraction gratings*, J. Opt. Soc. Am. A, 28 (2011), pp. 613–620.